Coupled Systems Mechanics, *Vol. 14, No. 4 (2025) 347-369*
https://doi.org/10.12989/csm.2025.14.4.347

Column buckling under stochastic three-dimensional material properties: A stochastic finite element analysis

Diem Dang Nguyen[1], Hien Duy Ta*[1], Dan Sy Dao[1] and Hung Duy Nguyen[2]

[1]*University of Transport and Communications, Ha Noi, Viet Nam*
[2]*Helmut Schmidt University/University of the Federal Armed Forces Hamburg, Germany*

(Received April 9, 2025, Revised July 20, 2025, Accepted August 22, 2025)

Abstract. This study develops a Stochastic Finite Element Analysis approach integrating a numerical integration method and a perturbation method to analyze the buckling response of columns subjected to three-dimensional (3D) stochastic material variations. The proposed method discretizes the 3D random field of Young's modulus into fundamental random variables. The method is further enhanced with perturbation techniques, supporting the estimation of important statistical descriptors, including the expected value, coefficient of variation (COV), and standard deviation of the critical buckling load. The accuracy of the Stochastic Finite Element Analysis is validated via Monte Carlo simulations (MCs) implemented with the conventional Finite Element Method (FEM), while spectral expansion techniques are employed to create random instances for the 3D stochastic field model. The results demonstrate that for small spatial correlation lengths, local material fluctuations are effectively averaged due to stochastic homogenization, leading to lower variability in the critical buckling load. Conversely, an expansion of the correlation length results in heightened variability in the critical load, reflecting the impact of stochastic variability of material properties. Among the spatial directions, the characteristic correlation distance along the column's longitudinal axis has the most significant influence on the uncertainty of the critical buckling load, as axial stiffness directly governs the global stability of the structure. Furthermore, the study reveals an approximately linear correlation between the COV of the critical buckling load and that of the elastic modulus, suggesting that material randomness can serve as a predictor of structural stability variability.

Keywords: buckling; elasticity; finite element method (FEM); stability; stochastic analysis

1. Introduction

The input factors for analyzing structural responses, such as the geometric dimensions of the structure, loads, and boundary conditions, are inherently uncertain and random (Troian 2023, Zhou *et al.* 2023, Zhao *et al.* 2024). These random input factors are typically represented mathematically as random variables or spatial random fields (Bastian and Rabitz 2020, Pulsipher *et al.* 2022, Wang *et al.* 2024). Consequently, random input factors result in structural responses that are also stochastic in nature. This necessitates analytical methods capable of quantifying and propagating randomness within the system for stochastic structural analysis. The Stochastic Finite Element

*Corresponding author, Associate Professor, E-mail: tdhien@utc.edu.vn

http://www.techno-press.org/?journal=csm&subpage=8 ISSN: 2234-2184 (Print), 2234-2192 (Online)

method (SFEM) integrates the standard finite element method (FEM) with stochastic computational theory, developed over recent decades to address the challenges of stochastic structural analysis (Johari and Talebi 2021, Saouma and Hariri-Ardebili 2021, Du *et al*. 2023).

Analyzing the stochastic response of structures using SFEM involves several key steps: representing random input factors as Gaussian or Non-Gaussian random fields, propagating randomness into the system, and performing stochastic response analysis (Nath *et al.* 2019, Sudret *et al.* 2020). SFEM methods can be broadly classified into two main categories. The first category comprises statistical SFEM approaches, which involve Monte Carlo simulations (MCs) of random field samples for the input factors, combined with standard FEM to produce datasets of stochastic structural responses (Hurtado and Barbat 1998, Schuëller and Pradlwarter 2007, Schuëller and Pradlwarter 2009). Although direct and robust, statistical methods demand large sample sizes, leading to significant computational time and increased costs (Arregui-Mena *et al.* 2016). The second category includes non-statistical approaches, particularly perturbation techniques (Elishakoff and Ren 2003, Ariaratnam & Schuëller 2020, Ta and Nguyen 2020) and spectral methods (Nouy 2009, Blatman and Sudret 2011, Pascual and Adhikari 2012). Perturbation-based non-statistical methods derive statistical descriptors of structural stochastic responses through Taylor series approximations of the structural response. On the other hand, spectral non-statistical methods represent the stochastic structural response as a perturbation series comprising eigenfunctions and random variables (Stefanou 2009).

Stability analysis of structures under compressive loads has been a topic of significant interest among researchers (Quang *et al.* 2020, Tien and Van 2023, Fonseca 2024, Lobo and Silva 2024, Najafian Jazi *et al*. 2024). Studies have primarily focused on reinforced concrete structures, steel structures, and composite materials, employing either experimental methods or theoretical approaches using programming tools or commercial software (Jamaluddin *et al*. 2013, Jiang *et al.* 2016, Cao *et al*. 2017, Ma *et al*. 2018, Yang *et al.* 2018, Jothimani and Umarani 2019). Material properties such as elastic modulus, Poisson's ratio, and shear modulus are often treated as random variables or uncertain parameters in stochastic structural response analysis (Fu *et al.* 2022, Das and Roy 2023, Zheng *et al*. 2024). For columns under compressive loads, the critical load is also uncertain when the material properties are random. Thus, determining the stochastic stability of columns plays a crucial role in enhancing the reliability of structural calculations and aligning computational models more closely with the physical problem (Krejsa and Kralik 2015, Hang *et al.* 2022, Zhao *et al*. 2024).

Ramu and Ganesan (1992) investigated the stability of columns with a one-dimensionally spatially varying stochastic elastic modulus along the column length under uniformly distributed random loads. The weighted integral technique was used to represent random fields, coupled with non-statistical SFEM based on perturbation methods to derive statistical descriptors of the critical load. For composite materials with unidirectional fiber reinforcement, Kowda (2002) conducted static and dynamic stability analyses of columns with both solid and thin-walled cross-sections. Random uncertainties in material properties, geometric dimensions, boundary conditions, and loads were incorporated into the analysis. Similarly, Ganesan and Kowda (2005) developed a non-statistical SFEM using perturbation techniques to analyze the stochastic stability of composite columns with randomly varying elastic moduli and cross-sectional widths. Their study focused on rectangular and thin-walled cross-sections. Expanding this research, Nguyen *et al.* (2017) applied spectral representation techniques to model random fields of material properties for fiber-reinforced composite columns. To perform stochastic analysis, the authors used MCs combined with the isoparametric finite element method to evaluate the stochastic stability of columns. The

stochastic stability problem was extended to cases involving non-Gaussian and non-homogeneous random fields Sasikumar *et al.* (2014), analyzing single-layer composite beams with spatially varying random elastic and shear moduli.

For columns with deterministic variations in cross-sectional geometry, Ta (2020) employed the weighted integral methods to represent random fields of elastic modulus varying along the column length. First-order perturbation techniques combined with SFEM were used to analyze static stochastic problems, yielding first-order statistical characteristics of displacements. Similarly, Hang *et al.* (2022) developed an SFEM based on perturbation techniques and random field point representation to analyze the stability of columns with linear variations in cross-sectional geometry along their length. In this study, the elastic modulus was modeled as a spatially varying random field along the column length. Beyond common random factors like material properties, cross-sectional dimensions, and loads, some studies have also considered initial column curvature as a random field (Kala *et al.* 2017). The authors analyzed the stability of columns with open and hollow sections, concluding that open cross-sections are more vulnerable to torsion compared to closed sections, which exhibit higher compressive strength. Stochastic stability analysis also includes the nonlinear interaction between loads and lateral deflection in the buckling of columns with spatially varying random elastic moduli (Ly *et al.* 2019).

Recent studies have increasingly focused on developing and applying the SFEM to enhance simulation accuracy and quantify uncertainties in engineering systems. Wu *et al.* (2023) proposed a homotopy-based SFEM model updating approach, incorporating the Karhunen–Loève expansion to process correlated static measurement data, ensuring consistency between model responses and experimental data. Meanwhile, Salazar and Hariri-Ardebili (2022) integrated machine learning with SFEM to evaluate heterogeneous concrete structures, using random forest models for sensitivity analysis and structural response prediction under dynamic loading. Additionally, Kamiński (2022) explored uncertainty analysis in solid mechanics using a perturbation-based SFEM with various probability distributions, such as uniform and triangular, to improve structural reliability assessments. In the field of geotechnical engineering, Chen *et al.* (2021) developed a three-dimensional SFEM model for large-deformation landslide simulations, incorporating spatial soil variability to enhance the accuracy of landslide extent and impact predictions. Similarly, Bozkurt *et al.* (2023) employed finite element analysis to assess the stability of deep excavations in soft clay reinforced with lime-cement columns, providing critical insights into safe construction practices in weak soil conditions. Yang *et al.* (2022) developed a bi-stage random field parameter estimation method for modeling geometric imperfections in cylindrical shells under limited data. In parallel, Liu *et al.* (2024) introduced a Bayesian deep learning approach using the computational fluid dynamics-based priors to improve wind power prediction in data-scarce environments. These works demonstrate the value of combining physical modeling and probabilistic inference to address spatial randomness and limited observations.

Despite significant advancements in research, the influence of three-dimensional (3D) stochastic variations in the elastic modulus on the critical load of compressed columns remains insufficiently explored. In particular, the impact of spatial correlation lengths in a 3D stochastic field on the uncertainty of the critical load remains an open question. To bridge this gap, this study develops the SFEM framework that integrates a weighted integration technique and perturbation methods to analyze the stability of compressed columns with a spatially varying stochastic Young's modulus. To enhance accuracy, the weighted quadrature method utilized to convert the 3D uncertain field into a discrete set of fundamental random variables. Subsequently, perturbation methods are employed to approximate the expansion series of the ultimate load, enabling the

estimation of key statistical parameters, including the expected value, coefficient of variation (COV), and the second central moment. The proposed SFEM is validated through MCs utilizing the standard FEM and 3D random field modeling. Additionally, the research examines the impact of critical uncertainty factors, such as spatial correlation lengths and material variability, on the buckling load. Finally, the relationship between the COV of Young's modulus and the COV of the instability load is systematically analyzed, providing valuable insights into the stochastic equilibrium of columns with 3D spatially varying material properties.

2. Random stability study of columns using SFEM

2.1 Determination of the buckling load of columns using FEM

Consider a centrally compressed column under the application of an axial force P. The column has a rectangular cross-section with a width b and a height h. To analyze the stability of the column using the standard FEM, the column is divided into N_e elements, where a represents the length of an element. The transverse deflection due to bending of each element is approximated using Hermite shape functions and the nodal displacement vector of the element, as given in Eq. (1). The shape function matrix is represented in Eq. (2)

$$v_e = [N]\{\delta\}_e \tag{1}$$

$$[N] = [N_1(x_e) \quad N_2(x_e) \quad N_3(x_e) \quad N_4(x_e)] = \underbrace{\begin{Bmatrix} x_e^0 \\ x_e^1 \\ x_e^1 \\ x_e^1 \end{Bmatrix}^T}_{\{r\}} \underbrace{\begin{bmatrix} 1 & 0 & 0 & 0 \\ 0 & 1 & 0 & 0 \\ -\frac{3}{a^2} & -\frac{2}{a} & \frac{3}{a^2} & -\frac{1}{a} \\ \frac{2}{a^3} & \frac{1}{a^2} & -\frac{2}{a^3} & \frac{1}{a^2} \end{bmatrix}}_{[\Gamma]} \tag{2}$$

For beam-column elements, the element stiffness matrix is determined by Eq. (3), comprising two components: Elastic stiffness matrix $[K]_e$, which accounts for the bending deformation, where $[B]$ is the strain-displacement matrix and E is the elastic modulus. Geometric stiffness matrix $[K_P]_e$, which captures the influence of axial compressive loads on the column's stiffness.

$$[k]_e = -P[K_P]_e + [K]_e \tag{3}$$

with

$$[K]_e = \int_{V_e} [B]^T [D][B] dV_e \tag{4}$$

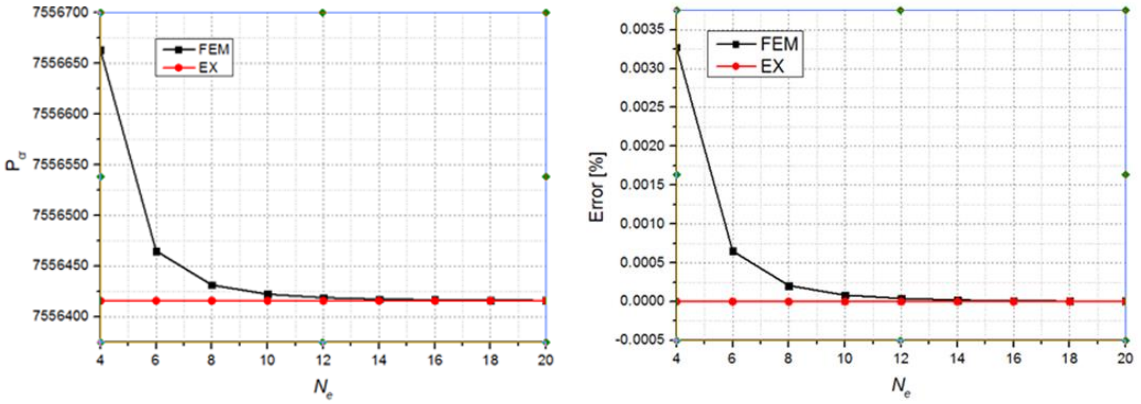

(a) Critical load determined by FEM and EX (b) Corresponding error

Fig. 1 Comparison of critical load determined by FEM and EX

$$[K_P]_e = \int_0^a [N']^T [N'] dx = \begin{bmatrix} \frac{6}{5a} & \frac{1}{10} & -\frac{6}{5a} & \frac{1}{10} \\ & \frac{2a}{15} & -\frac{1}{10} & -\frac{a}{30} \\ & & \frac{6}{5a} & -\frac{1}{10} \\ sym & & & \frac{2a}{15} \end{bmatrix} \tag{5}$$

The global stiffness matrix of the structure is assembled from the element stiffness matrices, as shown in Eq. (6)

$$[k] = \sum_{e=1}^{N_e} [k]_e = \underbrace{\sum_{e=1}^{N_e} [K]_e}_{[K]} - P \underbrace{\sum_{e=1}^{N_e} [K_P]_e}_{[K]_P} \tag{6}$$

In the context of standard FEM, the stability equation of the column is expressed as in Eq. (7), where $\{\Phi\}$ represents the buckling mode shape.

$$([K] - P[K]_P)\{\Phi\} = \{0\} \tag{7}$$

For Eq. (7) to have non-trivial solutions, the condition given in Eq. (8) must be satisfied. Solving Eq. (8) yields the critical load as the smallest eigenvalue

$$Det([K] - P[K]_P) = 0 \tag{8}$$

Fig. 1 presents the results of critical load analysis for a column with one fixed end and one free end. The column has the following parameters: length L=3.5 m, width b=0.35 m, height h=0.35 m, and elastic modulus E=30×10^3 Mpa. The critical load is determined using two methods: FEM and the exact solution (EX), with the number of elements varying from 4 to 20. The results are shown in Fig. 1(a), while the error between FEM and EX is displayed in Fig. 1(b). It can be

Table 1 Comparison between the Weighted Integral Method and Karhunen–Loève Expansion

Criterion	Weighted Integral Method	Karhunen–Loève Expansion (KLE)
Mathematical Foundation	Local averaging over element domains	Global spectral decomposition using eigenfunctions of covariance kernel
Computational Cost	Low to moderate (depends on number of integration points)	High (requires solving a large eigenvalue problem, especially in 3D)
Implementation Complexity	Relatively simple and mesh-independent	Complex, especially for irregular domains and high-dimensional fields
Accuracy (Mean-square optimality)	Not mean-square optimal; accuracy depends on integration scheme and mesh resolution	Mean-square optimal approximation for Gaussian fields
Mesh Compatibility	Fully compatible with arbitrary finite element meshes and shapes	Requires additional mapping for non-rectangular or unstructured meshes
Handling Short Correlation Lengths	Efficient; easily handles small correlation lengths through refined integration	Requires a large number of terms to capture short correlation structure
Scalability in 3D	Scales well with dimensionality	Computationally expensive in 3D problems due to high modal truncation requirements
Flexibility for Non-Gaussian Fields	Can be extended to some non-Gaussian fields via direct sampling	Primarily suited for Gaussian fields unless transformed or adapted

observed that as the number of elements increases, the buckling load computed using FEM approaches the exact solution derived analytically.

2.2 Development of the weighted integral technique for discretizing three-dimensional random fields

To discretize input random fields, several techniques have been proposed and developed, including: the random field point discretization techniques (Liu *et al*. 1986, Der Kiureghian and Ke 1988), the averaging discretization methods (Deodatis 1991, Van den Nieuwenhof and Coyette 2003), and the series expansion-based discretization approaches (Grigoriu 1993, Zhang and Ellingwood 1994). Among these, the weighted integral technique belongs to the averaging discretization group and offers the advantage of compatibility with any element mesh and correlation length of the uncertain field. In this work, we develop a weighted numerical integration scheme for discretizing the probabilistic field into fundamental random quantities. In this study, the weighted integral method is adopted to discretize the three-dimensional random field of material properties. To justify this choice, a concise comparison with the widely used Karhunen–Loève expansion (KLE) is presented in Table 1. The weighted integral method computes the stochastic stiffness matrix through numerical integration over each finite element, offering straightforward implementation and high compatibility with arbitrary meshes. It handles short correlation lengths efficiently and scales well in 3D. Conversely, KLE provides a mean-square optimal representation of Gaussian fields but requires solving a global eigenvalue problem, which becomes computationally intensive in three dimensions and for short correlation lengths. The main differences between the two methods are summarized in Table 1, highlighting their respective strengths and limitations in terms of mathematical formulation, computational efficiency, and practical applicability in SFEM (Der Kiureghian and Ke 1988, Deodatis 1991, Grigoriu 1993,

Zhang and Ellingwood 1994, Nouy 2009).

The elastic modulus of the column is considered as a three-dimensional spatially varying random field, expressed as in Eq. (9), where E_0 is the expected value of the elastic modulus, and $f(x_e, y_e, z_e)$ is a zero-mean, univariate, homogeneous three-dimensional random field.

$$E = E_0\left[1 + f\left(x_e, y_e, z_e\right)\right] \tag{9}$$

Substituting Eq. (9) into Eq. (4) yields Eq. (10)

$$[K]_e = \int_{V_e} [B]^T E_0 [B] dV_e + \int_{V_e} [B]^T E_0 f\left(x_e, y_e, z_e\right)[B] dV_e \tag{10}$$

The deformation-gradient matrix $[B]$ is specified as presented in Eq. (11)

$$[B] = -y_e [N''] \tag{11}$$

Substituting Eqs. (2) and (11) into Eq. (10) results in Eq. (12)

$$[K]_e = \underbrace{[\Gamma]^T \int_{V_e} E_0 y_e^2 [r'']^T [r''] dV_e [\Gamma]}_{[K_o]_e} + \underbrace{[\Gamma]^T \int_{V_e} E_0 y_e^2 f\left(x_e, y_e, z_e\right)[r'']^T [r''] dV_e [\Gamma]}_{[\Delta K]_e} \tag{12}$$

Considering Eq. (2), the term $[r'']^T[r'']$ appearing in Eq. (12) is determined as shown in Eq. (13)

$$[r'']^T [r''] = \begin{bmatrix} 0 & 0 & 0 & 0 \\ 0 & 0 & 0 & 0 \\ 0 & 0 & 4 & 12x_e \\ 0 & 0 & 12x_e & 36x_e^2 \end{bmatrix} \tag{13}$$

The stiffness matrix can be divided into two components: the deterministic part, given by Eq. (14), where I represents the second moment of area of the cross-section, and the random part, as shown in Eq. (15)

$$[K_0]_e = [\Gamma]^T \int_{V_e} E_0 y_e^2 [r'']^T [r''] dV_e [\Gamma] = \frac{E_0 I}{a^3} \begin{bmatrix} 12 & 6a & -12 & 6a \\ & 4a^2 & -6a & 2a^2 \\ & & 12 & -6a \\ sym & & & 4a^2 \end{bmatrix} \tag{14}$$

$$[\Delta K]_e = [\Gamma]^T \int_{V_e} E_0 y_e^2 f\left(x_e, y_e, z_e\right)[r'']^T [r''] dV_e [\Gamma] \tag{15}$$

Substituting Eq. (13) into Eq. (15), the random component of the stiffness matrix can be rewritten as Eq. (16), with the matrices involved defined in Eqs. (17)-(19)

$$\begin{aligned} [\Delta K]_e = {} & [\Delta K_1]_e \int_{V_e} y_e^2 f\left(x_e, y_e, z_e\right) dV_e + [\Delta K_2]_e \int_{V_e} x_e y_e^2 f\left(x_e, y_e, z_e\right) dV_e \\ & + [\Delta K_3]_e \int_{V_e} x_e^2 y_e^2 f\left(x_e, y_e, z_e\right) dV_e \end{aligned} \tag{16}$$

$$[\Delta K_1]_e = \frac{E_0}{a^6}\begin{bmatrix} 36a^2 & 24a^3 & -36a^2 & 12a^3 \\ & 16a^4 & -24a^3 & 8a^4 \\ & & 36a^2 & -12a^3 \\ sym & & & 4a^4 \end{bmatrix} \tag{17}$$

$$[\Delta K_2]_e = \frac{E_0}{a^6}\begin{bmatrix} -144a & -84a^2 & 144a & -60a^2 \\ & -48a^3 & 84a^2 & -36a^3 \\ & & -144a & 60a^2 \\ sym & & & -24a^3 \end{bmatrix} \tag{18}$$

$$[\Delta K_3]_e = \frac{E_0}{a^6}\begin{bmatrix} 144 & 72a & -144 & 72a \\ & 36a^2 & -72a & 36a^2 \\ & & 144 & -72a \\ sym & & & 36a^2 \end{bmatrix} \tag{19}$$

The fundamental random variables are defined as shown in Eq. (20)

$$\mathrm{X}_i^e = \int_{V_e} x_e^{i-1} y_e^2 f(x_e, y_e, z_e)\, dV_e \qquad i = 1,2,3 \tag{20}$$

Substituting Eq. (20) into Eq. (16) yields Eq. (21)

$$[\Delta K]_e = [\Delta K_1]_e \mathrm{X}_1^e + [\Delta K_2]_e \mathrm{X}_2^e + [\Delta K_2]_e \mathrm{X}_3^e = \sum_{i=1}^{3} [\Delta K_i]_e \mathrm{X}_i^e \tag{21}$$

2.3 Stochastic critical load analysis using SFEM with perturbation technique

The SFEM based on the perturbation technique falls within the class of non-statistical methods, which is suitable for linear analysis, nonlinear analysis, time-dependent analysis, and eigenvalue problems (Arregui-Mena *et al*. 2016). In this study, the authors developed an SFEM approach combining the perturbation technique with the discretization of random fields using weighted integral techniques to analyze the stochastic stability of columns. It is important to note that the perturbation-based stochastic finite element method (SFEM) employed in this study is based on the assumption of small randomness in the input parameters. Specifically, the coefficient of variation (COV) of the spatially varying elastic modulus must be sufficiently low (Elishakoff and Ren 2003, Nouy 2009, Stefanou 2009) to ensure the accuracy of the first-order Taylor series expansion. This small-perturbation assumption allows the truncation of higher-order terms while maintaining acceptable approximation errors in the evaluation of statistical moments of the critical buckling load. Therefore, the applicability of the proposed method is limited to structural systems where the stochastic variability of material properties remains within a moderate range.

Substituting Eqs. (6), (12), and (21) into Eq. (7) yields the stability equation for the column, expressed as Eq. (22)

$$\left[\underbrace{\sum_{e=1}^{N_e}[K_0]_e}_{[K_0]}+\sum_{e=1}^{N_e}\sum_{i=1}^{3}[\Delta K_i]_e \mathrm{X}_i^e - P[K]_P\right]\{\Phi\}=\{0\} \tag{22}$$

Let $\lambda_i = P$ denote the eigenvalue corresponding to the critical load. The stability equation associated with the *k*-th eigenvalue is rewritten as Eq. (23)

$$\left[\underbrace{\left([K_0]+\sum_{e=1}^{N_e}\sum_{i=1}^{3}[\Delta K_i]_e \mathrm{X}_i^e\right)}_{[K]} - \lambda_k [K]_P\right]\{\Phi_k\}=\{0\} \tag{23}$$

Since the random variables $\{X\}=\{X_i^e\}_{i=1,2,3}^{e=1:N_e}$ are discretized from a random field with zero mean, their expected values are also zero. Applying the perturbation method to approximate the quantities in Eq. (23) as series expansions results in Eqs. (24)-(26), with the first-order and second-order partial derivatives evaluated at $\{X\}=\{0\}$

$$[K]=[K_0]+\sum_{e=1}^{N_e}\sum_{i=1}^{3}\frac{\partial[K]}{\partial \mathrm{X}_i^e}\mathrm{X}_i^e+\sum_{e_1=1}^{N_e}\sum_{i_1}^{3}\sum_{e_2=1}^{N_e}\sum_{i_2=1}^{3}\frac{\partial^2[K]}{\partial \mathrm{X}_{i_1}^{e_1}\partial \mathrm{X}_{i_2}^{e_2}}\mathrm{X}_{i_1}^{e_1}\mathrm{X}_{i_2}^{e_2}+\ldots \tag{24}$$

$$\lambda_k=\lambda_k^0+\sum_{e=1}^{N_e}\sum_{i=1}^{3}\frac{\partial\lambda_k}{\partial \mathrm{X}_i^e}\mathrm{X}_i^e+\sum_{e_1=1}^{N_e}\sum_{i_1}^{3}\sum_{e_2=1}^{N_e}\sum_{i_2=1}^{3}\frac{\partial^2\lambda_k}{\partial \mathrm{X}_{i_1}^{e_1}\partial \mathrm{X}_{i_2}^{e_2}}\mathrm{X}_{i_1}^{e_1}\mathrm{X}_{i_2}^{e_2}+\ldots \tag{25}$$

$$\{\Phi_k\}=\{\Phi_k^0\}+\sum_{e=1}^{N_e}\sum_{i=1}^{3}\frac{\partial\{\Phi_k\}}{\partial \mathrm{X}_i^e}\mathrm{X}_i^e+\sum_{e_1=1}^{N_e}\sum_{i_1}^{3}\sum_{e_2=1}^{N_e}\sum_{i_2=1}^{3}\frac{\partial^2\{\Phi_k\}}{\partial \mathrm{X}_{i_1}^{e_1}\partial \mathrm{X}_{i_2}^{e_2}}\mathrm{X}_{i_1}^{e_1}\mathrm{X}_{i_2}^{e_2}+\ldots \tag{26}$$

Substituting Eqs. (24)-(26) into Eq. (23) and collecting terms of the same order of partial derivatives yield the following Eqs. (27)-(28):

Zero-order

$$\left[[K_0]-\lambda_k^0[K_P]\right]\{\Phi_k^0\}=\{0\} \tag{27}$$

First-order

$$\left[[K_0]-\lambda_k^0[K_P]\right]\sum_{e=1}^{N_e}\sum_{i=1}^{3}\frac{\partial\{\Phi_k\}}{\partial \mathrm{X}_i^e}=\left[[K_P]\sum_{e=1}^{N_e}\sum_{i=1}^{3}\frac{\partial\lambda^k}{\partial \mathrm{X}_i^e}-\sum_{e=1}^{N_e}\sum_{n=1}^{N_w}\frac{\partial[K]}{\partial \mathrm{X}_i^e}\right]\{\Phi_k^0\} \tag{28}$$

Taking the partial derivative of Eq. (23) with respect to the random variables X_i^e and considering Eqs. (27)-(28), results in Eq. (29)

$$\frac{\partial\lambda_k}{\partial \mathrm{X}_i^e}=\frac{\{\Phi_k^0\}^T\dfrac{\partial[K]}{\partial \mathrm{X}_i^e}\{\Phi_k^0\}}{\{\Phi_k^0\}^T[K_P]\{\Phi_k^0\}} \tag{29}$$

Substituting Eq. (29) into Eq. (25) , we obtain Eq. (30)

$$\lambda_k = \lambda_k^0 + \sum_{e=1}^{N_e}\sum_{i=1}^{3} \frac{\left\{\Phi_k^0\right\}^T \dfrac{\partial[K]}{\partial \mathrm{X}_i^e}\left\{\Phi_k^0\right\}}{\left\{\Phi_k^0\right\}^T [K_P]\left\{\Phi_k^0\right\}} \mathrm{X}_i^e \tag{30}$$

Calculating the distributional properties of the ultimate load eigenvalue, as described in Eqs. (31)-(33)

$$E[\lambda_k] = E\left[\lambda_k^0 + \sum_{e=1}^{N_e}\sum_{i=1}^{3} \frac{\left\{\Phi_k^0\right\}^T \dfrac{\partial[K]}{\partial \mathrm{X}_i^e}\left\{\Phi_k^0\right\}}{\left\{\Phi_k^0\right\}^T [K_P]\left\{\Phi_k^0\right\}} \mathrm{X}_i^e\right] \approx \lambda_k^0 \tag{31}$$

$$\mathrm{Var}[\lambda_k] = E\left[\left(\lambda_k - E[\lambda_k]\right)\left(\lambda_k - E[\lambda_k]\right)^T\right] \tag{32}$$

Substituting Eq. (30) into Eq. (32) yields Eq. (33)

$$\mathrm{Var}[\lambda_k] = \sum_{e_1=1}^{N_e}\sum_{i_1=1}^{3}\sum_{e_2=1}^{N_e}\sum_{i_2=1}^{3} \frac{\left\{\Phi_k^0\right\}^T \dfrac{\partial[K]}{\partial \mathrm{X}_{i_1}^{e_1}}\left\{\Phi_k^0\right\}\left\{\Phi_k^0\right\}^T \dfrac{\partial[K]}{\partial \mathrm{X}_{i_2}^{e_2}}\left\{\Phi_k^0\right\}}{\left\{\Phi_k^0\right\}^T [K_P]\left\{\Phi_k^0\right\}\left\{\Phi_k^0\right\}^T [K_P]\left\{\Phi_k^0\right\}} E\left[\mathrm{X}_{i_1}^{e_1}\mathrm{X}_{i_2}^{e_2}\right] \tag{33}$$

Based on Eq. (20), the expectation term in Eq. (33) can be reformulated as shown in Eq. (34)

$$E\left[\mathrm{X}_{i_1}^{e_1}\mathrm{X}_{i_2}^{e_2}\right] = \int_{V_{e_1}}\int_{V_{e_2}} x_{e_1}^{i_1-1} y_{e_1}^2 x_{e_2}^{i_2-1} y_{e_2}^2 E\left[f\left(x_{e_1}, y_{e_1}, z_{e_1}\right) f\left(x_{e_2}, y_{e_2}, z_{e_2}\right)\right] dV_{e_1} dV_{e_2} \tag{34}$$

The expected value of the product of random fields at any two elements is determined using the correlation function of the random field, as defined in Eq. (35). The autocorrelation function (R_{ff}) quantifies the degree of statistical dependence between spatial points in the field, thereby capturing the underlying structure of material heterogeneity. It reflects how variations at one location influence those at another, and plays a crucial role in the accurate estimation of variance and other second-order statistical moments in stochastic finite element analysis.

$$E\left[f\left(x_{e_1}, y_{e_1}, z_{e_1}\right) f\left(x_{e_2}, y_{e_2}, z_{e_2}\right)\right] = R_{ff} \tag{35}$$

Substituting Eq. (35) into Eq. (34) yields Eq. (36)

$$E\left[\mathrm{X}_{i_1}^{e_1}\mathrm{X}_{i_2}^{e_2}\right] = \int_{V_{e_1}}\int_{V_{e_2}} x_{e_1}^{i_1-1} y_{e_1}^2 x_{e_2}^{i_2-1} y_{e_2}^2 R_{ff}\, dV_{e_1} dV_{e_2} \tag{36}$$

Substituting Eq. (36) into Eq. (33) yields Eq. (37)

$$\mathrm{Var}[\lambda_k] = \sum_{e_1=1}^{N_e}\sum_{i_1=1}^{3}\sum_{e_2=1}^{N_e}\sum_{i_2=1}^{3} \left\{ \begin{array}{l} \dfrac{\left\{\Phi_k^0\right\}^T \dfrac{\partial[K]}{\partial \mathrm{X}_{i_1}^{e_1}}\left\{\Phi_k^0\right\}\left\{\Phi_k^0\right\}^T \dfrac{\partial[K]}{\partial \mathrm{X}_{i_2}^{e_2}}\left\{\Phi_k^0\right\}}{\left\{\Phi_k^0\right\}^T [K_P]\left\{\Phi_k^0\right\}\left\{\Phi_k^0\right\}^T [K_P]\left\{\Phi_k^0\right\}} \times \\ \displaystyle\int_{V_{e_1}}\int_{V_{e_2}} x_{e_1}^{i_1-1} y_{e_1}^2 x_{e_2}^{i_2-1} y_{e_2}^2 R_{ff}\, dV_{e_1} dV_{e_2} \end{array} \right\} \tag{37}$$

Since the matrix [*K*] is a linear function of the random variables, its first-order partial derivatives can be determined as shown in Eq. (38), where $[[\Delta K_i]_e]_E$ is an extended matrix of the same size as [*K*], with zero values in the extended elements

$$\frac{\partial[K]}{\partial X_i^e} = \left[\left[\Delta K_i\right]_e\right]_E \tag{38}$$

Substituting Eq. (38) into Eq. (37) gives Eq. (39)

$$\mathrm{Var}[\lambda_k] = \sum_{e_1=1}^{N_e}\sum_{i_1=1}^{3}\sum_{e_2=1}^{N_e}\sum_{i_2=1}^{3}\left\{\begin{array}{l}\dfrac{\left\{\Phi_k^0\right\}^T\left[\left[\Delta K_{i_1}\right]_{e_1}\right]_E\left\{\Phi_k^0\right\}\left\{\Phi_k^0\right\}^T\left[\left[\Delta K_{i_2}\right]_{e_2}\right]_E\left\{\Phi_k^0\right\}}{\left\{\Phi_k^0\right\}^T[K_P]\left\{\Phi_k^0\right\}\left\{\Phi_k^0\right\}^T[K_P]\left\{\Phi_k^0\right\}}\times \\ \displaystyle\int_{V_{e_1}}\int_{V_{e_2}} x_{e_1}^{i_1-1}y_{e_1}^2 x_{e_2}^{i_2-1}y_{e_2}^2 R_{ff}\,dV_{e_1}dV_{e_2}\end{array}\right\} \tag{39}$$

The coefficient of variation (COV) of the buckling load is determined using Eq. (40)

$$\mathrm{COV} = \frac{\sqrt{\mathrm{Var}[\lambda_k]}}{E[\lambda_k]} \tag{40}$$

3. Computational results and discussion

3.1 Verification of analysis results

An independent method has been developed based on Monte Carlo simulations to validate the SFEM solution proposed in this study. The 3D uncertain elastic modulus field is represented by *N* sample functions using the spectral representation method (Shinozuka and Deodatis 1991, Shinozuka and Deodatis 1996). Stability analysis of the column is performed using FEM on the set of *N* sample functions, yielding *N* values of the critical load. The obtained data is then analyzed to derive statistical descriptors of the buckling load. For the three-dimensional, stationary, zero-mean Gaussian random field, represented using spectral methods, the stochastic field is represented as a finite summation of harmonic functions, with the initial phases being random variables as shown in Eq. (41).

$$f(x,y,z) = \sqrt{2}\sum_{n_1=0}^{N_1-1}\sum_{n_2=0}^{N_2-1}\sum_{n_3=0}^{N_3-1}\left\{\begin{array}{l} A_{n_1n_2n_3}^{(1f)}\cos\left[\Omega_{1n_1}^f x+\Omega_{2n_2}^f y+\Omega_{3n_3}^f z+\Phi_{n_1n_2n_3}^{(1f)}\right] \\ +A_{n_1n_2n_3}^{(2f)}\cos\left[\Omega_{1n_1}^f x+\Omega_{2n_2}^f y-\Omega_{3n_3}^f z+\Phi_{n_1n_2n_3}^{(2f)}\right] \\ +A_{n_1n_2n_3}^{(3f)}\cos\left[\Omega_{1n_1}^f x-\Omega_{2n_2}^f y+\Omega_{3n_3}^f z+\Phi_{n_1n_2n_3}^{(3f)}\right] \\ +A_{n_1n_2n_3}^{(4f)}\cos\left[\Omega_{1n_1}^f x-\Omega_{2n_2}^f y-\Omega_{3n_3}^f z+\Phi_{n_1n_2n_3}^{(4f)}\right]\end{array}\right\} \tag{41}$$

where

$$A_{0n_2n_3}^{(if)} = A_{n_10n_3}^{(if)} = A_{n_1n_20}^{(if)} = 0 \qquad ;i=1,2,3,4 \tag{42}$$

$\Phi_{n_1 n_2 n_3}^{(if)}$ represents independent, uniformly distributed random variables in $[0 \quad 2\pi]$. In Eq. (41) the coefficients $A_{n_1 n_2 n_3}^{(if)}$ are defined as follows

$$A_{n_1 n_2 n_3}^{(1f)} = \sqrt{2S_{ff}\left(\Omega_{1n_1}^f, \Omega_{2n_2}^f, \Omega_{3n_3}^f\right)\Delta\Omega_1^f \Delta\Omega_2^f \Delta\Omega_3^f} \tag{43}$$

$$A_{n_1 n_2 n_3}^{(2f)} = \sqrt{2S_{ff}\left(\Omega_{1n_1}^f, \Omega_{2n_2}^f, -\Omega_{3n_3}^f\right)\Delta\Omega_1^f \Delta\Omega_2^f \Delta\Omega_3^f} \tag{44}$$

$$A_{n_1 n_2 n_3}^{(3f)} = \sqrt{2S_{ff}\left(\Omega_{1n_1}^f, -\Omega_{2n_2}^f, \Omega_{3n_3}^f\right)\Delta\Omega_1^f \Delta\Omega_2^f \Delta\Omega_3^f} \tag{45}$$

$$A_{n_1 n_2 n_3}^{(4f)} = \sqrt{2S_{ff}\left(\Omega_{1n_1}^f, -\Omega_{2n_2}^f, -\Omega_{3n_3}^f\right)\Delta\Omega_1^f \Delta\Omega_2^f \Delta\Omega_3^f} \tag{46}$$

$\Omega_{in_i}^f$ in Eqs. (40)-(43) are further determined by the Eqs. (47)-(49)

$$\Omega_{1n_1}^f = n_1 \Delta\kappa_1^f \qquad n_1 = 1, 2, ..., N_1 - 1 \tag{47}$$

$$\Omega_{2n_2}^f = n_2 \Delta\Omega_2^f \qquad n_2 = 1, 2, ..., N_2 - 1 \tag{48}$$

$$\Omega_{3n_3}^f = n_3 \Delta\Omega_3^f \qquad n_3 = 1, 2, ..., N_3 - 1 \tag{49}$$

$\Delta\Omega_i^f$ in Eqs. (40)-(43) are further determined by the Eq. (50)

$$\Delta\Omega_1^f = \frac{\Omega_{1u}^f}{N_1} \quad ; \quad \Delta\Omega_2^f = \frac{\Omega_{2u}^f}{N_2} \quad ; \quad \Delta\Omega_3^f = \frac{\Omega_{3u}^f}{N_3} \tag{50}$$

The power spectral density function of the three-dimensional, univariate, homogeneous, zero-mean Gaussian random field used in Eqs. (43)-(46) is written as

$$S_{ff}\left(\Omega_1^f, \Omega_2^f, \Omega_3^f\right) = \sigma_f^2 \frac{d_x d_y d_z}{8\pi^{1.5}} \exp\left[-\left(\frac{d_x \Omega_1^f}{2}\right)^2 - \left(\frac{d_y \Omega_2^f}{2}\right)^2 - \left(\frac{d_z \Omega_3^f}{2}\right)^2\right] \tag{51}$$

where σ_f is the root mean square deviation of the random elastic modulus field. d_x, d_y, and d_z denote the characteristic correlation lengths along the x, y, and z directions, respectively.

Consider a compression column with dimensions: L=3.5 m, b=h=0.35 m, and the elastic modulus of the column, which varies randomly in three dimensions, E_0=30×10^3 Mpa. To ensure the numerical accuracy and stability of the proposed SFEM framework, a mesh convergence analysis was carried out using three levels of discretization with 10, 20, and 30 beam-column elements (N_e), corresponding to four boundary condition cases at both ends of the column: column with both ends fixed (C–C), column with both ends hinged (H–H), column with one end fixed and one end hinged (C–H), and column fixed at one end and free at the other (C–F), where σ_f=0.05. The COV of the critical buckling load was adopted as the convergence criterion, as it directly reflects the variability in the structural response due to material uncertainty. As shown in Figs. 2(a)-(d), the COV decreases insignificantly when the number of elements increases from 10 to 20, and exhibits negligible change beyond 30 elements. This behavior indicates that the numerical

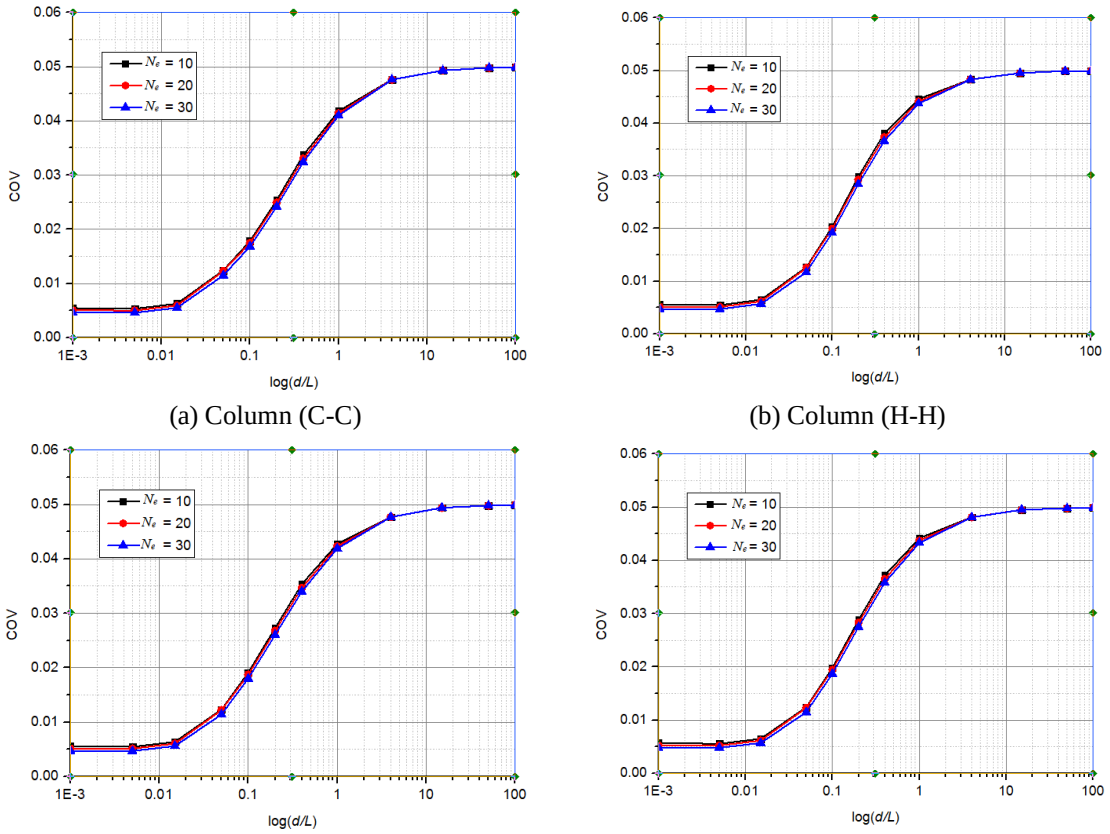

(a) Column (C-C) (b) Column (H-H)

(c) Column (C-H) (d) Column (C-F)

Fig. 2 Mesh convergence analysis of the stochastic finite element method

solution becomes stable and insensitive to further mesh refinement at this level. Therefore, a mesh of 30 elements is employed in all subsequent simulations to balance computational cost and solution accuracy.

Fig. 3 (a)-(d) present a comparison of the COV of the ultimate load, determined using two distinct approaches: the statistical approach (MCs) and the non-statistical approach (SFEM). The correlation lengths in 3D space are taken to be equal and vary within the range of 0.001 L to 100 L. The analysis results indicate that the COV estimated using SFEM closely matches the COV derived from the statistical approach based on Monte Carlo simulations. Significantly, when the characteristic correlation length is large, the COV determined by both methods does not differ significantly. The comparative analysis results confirm the reliability and precision of the SFEM solution proposed in this study for the stochastic stability assessment of the column.

3.2 Analysis of the effect of three-dimensional random field factors on COV

To examine the effect of spatial correlation lengths on the COV of the critical buckling load, three cases are examined: the first case, where the COV depends on d_x, d_y, and d_z with d_y=d_z; the second case, where the COV depends on d_x, d_y, and d_z with d_x=d_z; and the third case, where the

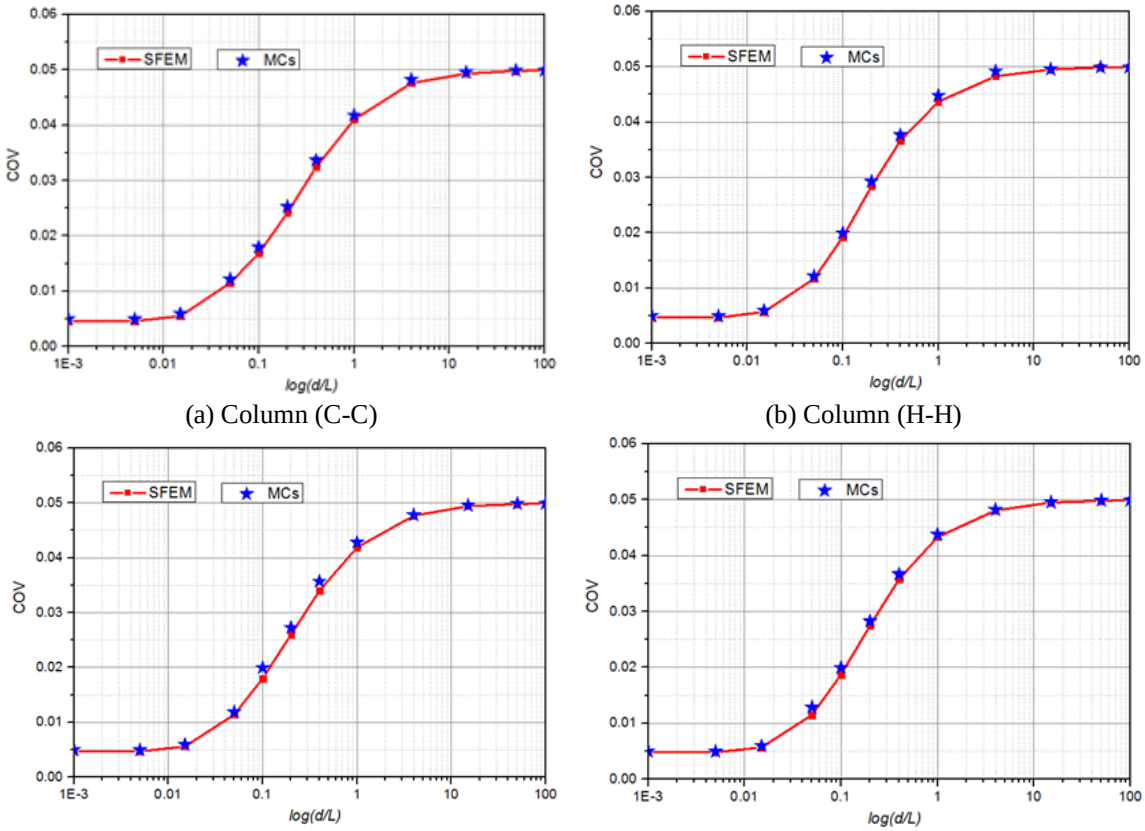

(a) Column (C-C) (b) Column (H-H)

(c) Column (C-H) (d) Column (C-F)

Fig. 3 Analysis of COV results from SFEM and MCs

COV depends on d_x,d_y, and d_z with d_x=d_y. Four boundary condition cases at both ends of the column are considered, and the correlation lengths along the axes are varied from 0.001 L to 100 L. Figs. 4-6 illustrate the dependence of the COV on correlation lengths in three-dimensional space.

For shorter characteristic correlation lengths, the COV of the buckling load is small, whereas it increases with longer spatial characteristic correlation lengths. In other words, when the spatial characteristic correlation lengths along the axes are small, the ultimate load exhibits slight fluctuations around its mean value, resulting in low dispersion. However, as the characteristic correlation length grows, the variation in the critical load also rises due to the local homogeneity of the elastic modulus over larger regions. When the characteristic correlation length attains a sufficiently large magnitude, the COV of the ultimate load is progressively increasing, but at an insignificant rate.

Notably, the characteristic length of correlation along the *x*-axis, which aligns with the column length, has a more dominant influence on the COV compared to the other axes. This indicates that the variation in the elastic modulus in the axial direction has a stronger effect on the stability of the column than variations in the transverse directions. This can be explained by the fact that fluctuations in the elastic modulus $E(x,y,z)$ along the *x*-axis directly affect the overall stiffness of

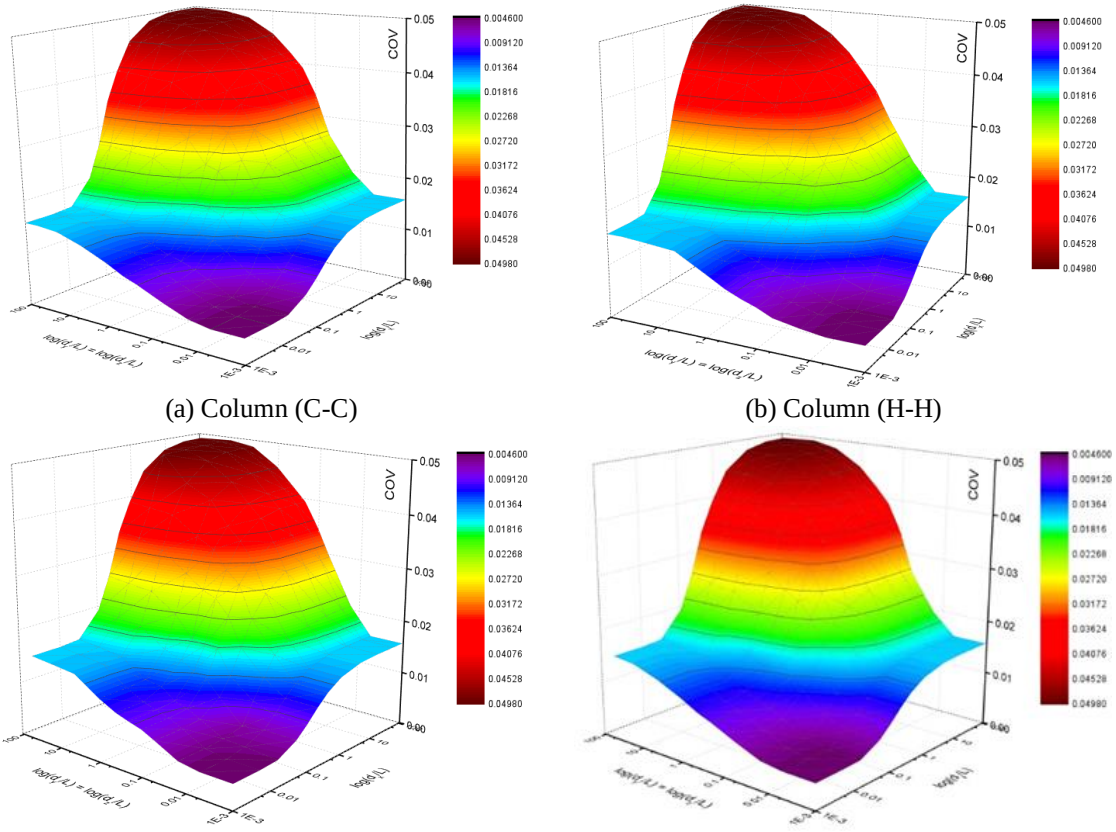

(a) Column (C-C) (b) Column (H-H)

(c) Column (C-H) (d) Column (C-F)

Fig. 4 COV dependence on correlation distances in three-dimensional space (d_y=d_z, σ_f=0.05)

the column, thereby significantly influencing its compressive capacity and critical load. In contrast, variations along the *y*- and *z*-axes primarily impact the cross-sectional properties of the column, resulting in more localized effects with less influence on overall structural stability.

This study investigates the outcome of the root mean square deviation on the COV of the ultimate load as shown in Fig. 7 (a)-(d), considering σ_f values of 0.05, 0.10, 0.15, and 0.20. The findings suggest a direct correlation between σ_f and COV, indicating that as σ_f increases, the COV of the ultimate load also rises. This phenomenon occurs because the randomness of the elastic modulus directly influences the overall stiffness of the column, altering the ultimate load value. When the dispersion of the Young's modulus is significant, the local variation in structural stiffness increases, leading to greater dispersion in the ultimate load.

Furthermore, the correlation between the COV of the ultimate load and σ_f is also governed by the correlation length of the random field. When the correlation length is small, the elastic modulus fluctuates rapidly in space, resulting in an even distribution of weak and strong material regions throughout the structure. This averaging effect reduces fluctuations in the critical load around its mean value, leading to a lower COV. In contrast, when the correlation length is large, regions with similar elastic modulus extend over a wider area, increasing the likelihood of localized weak or strong zones. This, in turn, enhances the variation in the critical load, resulting

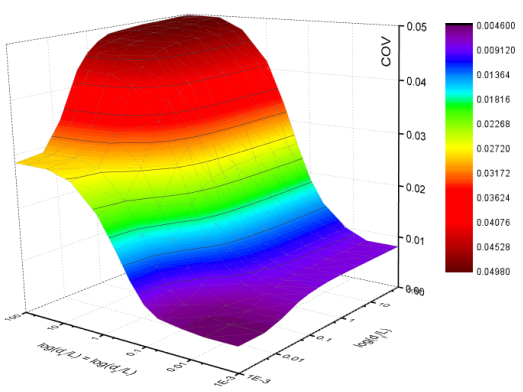

(a) Column (C-C)

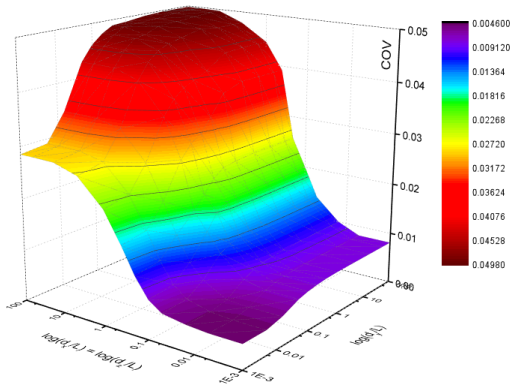

(b) Column (H-H)

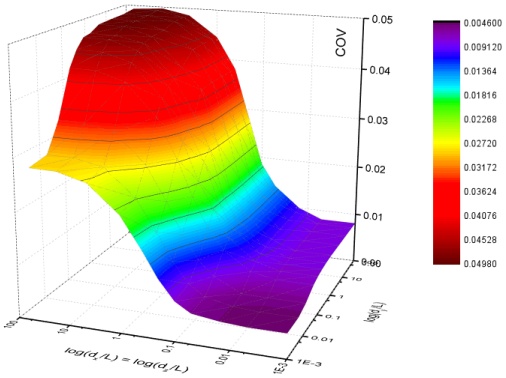

(c) Column (C-H)

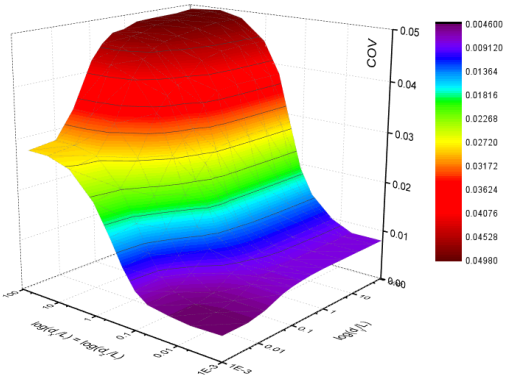

(d) Column (C-F)

Fig. 5 COV dependence on correlation distances in three-dimensional space (d_x=d_y, σ_f=0.05)

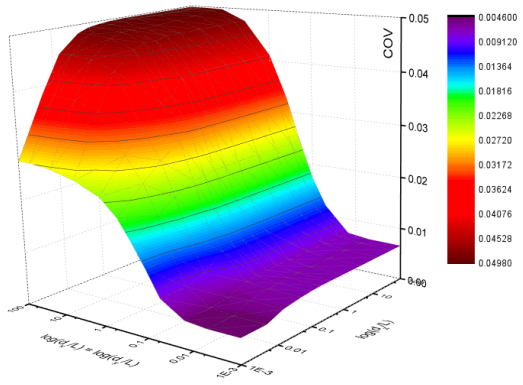

(a) Column (C-C)

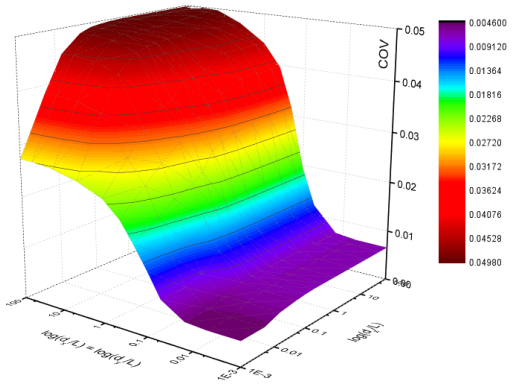

(b) Column (H-H)

Fig. 6 COV dependence on correlation distances in three-dimensional space (d_x=d_y, σ_f=0.05)

in a higher COV. Interestingly, as the characteristic correlation lengths asymptotically increases, The COV the COV tends to converge to σ_f, as the influence of local randomness diminishes and the material properties become more uniform throughout the structure.

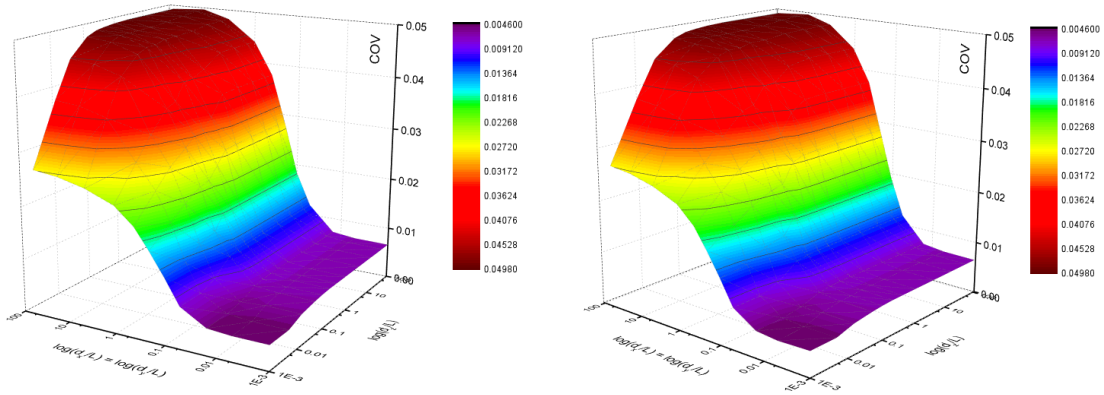

(c) Column (C-H) (d) Column (C-F)

Fig. 6 Continued

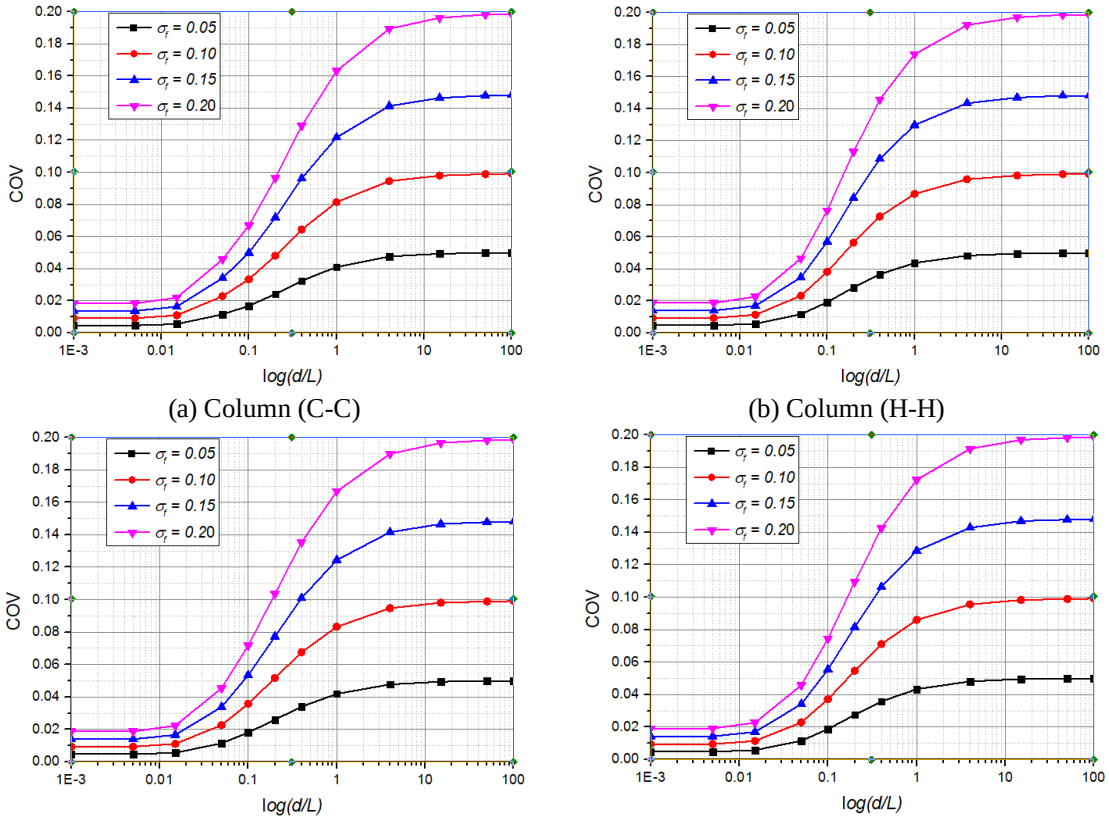

(a) Column (C-C) (b) Column (H-H)

(c) Column (C-H) (d) Column (C-F)

Fig. 7 Effect of σ_f on COV

A detailed investigation has been conducted to examine how increasing material randomness, represented by the COV of the elastic modulus, affects the variability of the critical buckling load. The numerical results reveal a clear trend: as the COV increases, the dispersion in the critical load

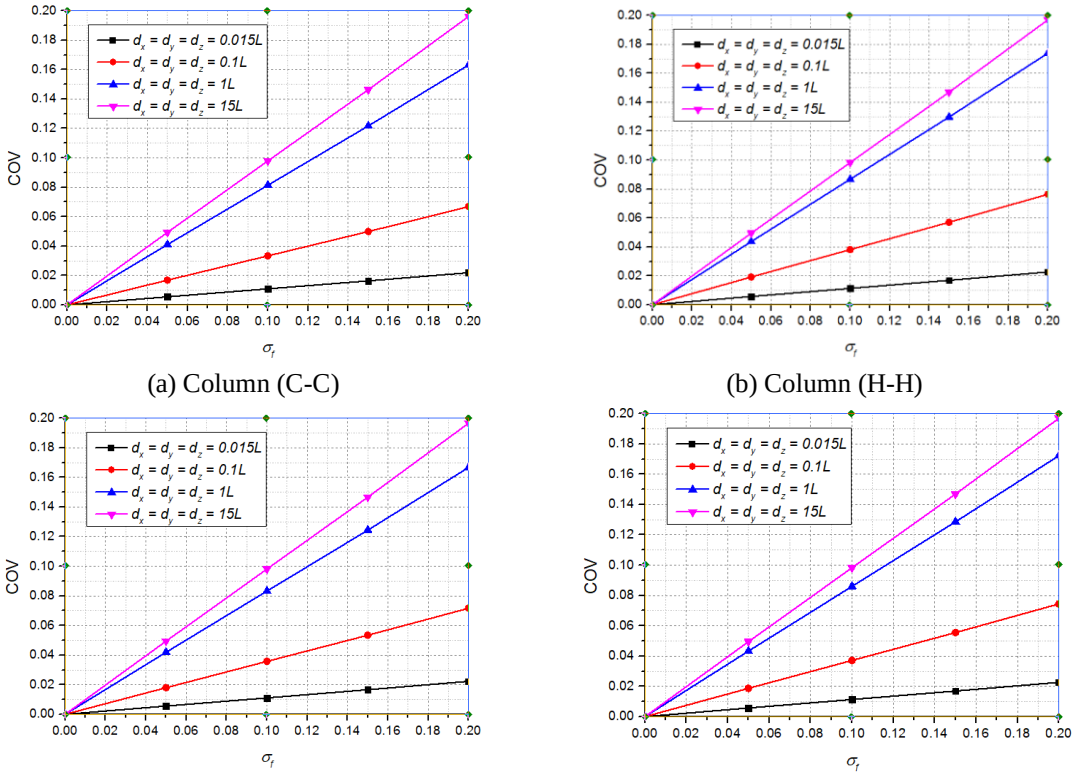

(a) Column (C-C) (b) Column (H-H)

(c) Column (C-H) (d) Column (C-F)

Fig. 8 Relationship between COV and σ_f

correspondingly increases, reflecting the growing influence of spatial uncertainty in material stiffness. This observation is consistent across different boundary condition scenarios and spatial correlation lengths. The findings provide valuable insight into the practical limits of the perturbation-based SFEM. Specifically, when the COV remains within a moderate range (typically ≤0.2), the proposed framework maintains high accuracy and numerical stability. However, beyond this range, the effect of higher-order terms may become significant, suggesting the need for more advanced techniques such as higher-order perturbation expansions or non-intrusive stochastic methods.

The association between the COV of the ultimate load and the variability of the 3D elastic modulus reflects the extent to which material randomness influences the stability response of the structure. To analyze this relationship, the study considers multiple cases with different correlation distances. Additionally, σ_f is selected with values 0.00, 0.05, 0.10, 0.15, and 0.20 to assess the impact of material variability on the critical load. The results of the analysis, as illustrated in Fig. 8 (a)-(d), indicate that the COV of the ultimate load demonstrates a close to linear correlation with the COV of the elastic modulus. This implies that once the random properties of the elastic modulus are known, the extent of the dispersion of the ultimate load can be predicted without the need for extensive random simulations.

This linear relationship has significant implications for stability analysis and the design of load-bearing structures, particularly in systems utilizing highly random materials such as composite

structures, biological materials, or fiber-reinforced concrete. Understanding the variability of the elastic modulus allows for the prediction of the dispersion range of the critical load, thereby enhancing the reliability and safety of structures. The approximately linear relationship observed in Fig. 8 between the coefficient of variation (COV) of the elastic modulus and that of the critical buckling load can be theoretically explained using first-order perturbation expansion. In stochastic finite element analysis, when the material randomness is sufficiently small, the structural response can be approximated as a smooth function of the input random variables. Under this assumption, the variation in the output becomes linearly dependent on the variation in the input. Specifically, if the elastic modulus exhibits weak randomness, the perturbation approximation indicates that the COV of the output response (the critical buckling load) is approximately proportional to the COV of the input property. This theoretical insight supports the observed numerical trend and is consistent with previous studies on perturbation-based stochastic finite element methods, such as those by Elishakoff and Ren (2003), Stefanou (2009).

Furthermore, this result facilitates the optimization of stochastic analysis, reducing the number of simulations required while maintaining high accuracy in structural response prediction. This is particularly valuable in engineering practice, where minimizing computational costs while ensuring accuracy is a crucial requirement.

4. Conclusions

This study successfully developed the stochastic finite element framework incorporating the perturbation method and the weighted numerical integration method to examine the buckling behavior of columns with a 3D stochastic Young's modulus field. The developed method was thoroughly verified by means of comparisons with MCs, demonstrating strong agreement between results and confirming its accuracy.

The study highlights the critical influence of spatial material randomness on the variability of the critical buckling load. The findings indicate that when the correlation length of the random field is small, local random fluctuations in material properties are effectively averaged, resulting in lower variability in the critical load. Conversely, as the characteristic correlation lengths increase, the dispersion of the ultimate load becomes more significant, reflecting the growing impact of large-scale material heterogeneities.

Among the spatial directions, the correlation length along the column's axial direction plays a dominant role in governing uncertainty in the critical load, as variations in axial stiffness directly affect the global stability of the structure. In contrast, variations in transverse directions predominantly influence localized stress redistribution, contributing less to overall buckling behavior.

A key theoretical insight derived from this study is that as the characteristic correlation lengths increase without bound, the COV of the ultimate load gradually aligns with the variability of the 3D uncertain field. Additionally, the study establishes an approximately linear correlation between the COV of the modulus of elasticity and the COV of the ultimate load, providing a predictive tool for assessing the stochastic stability of columns.This relationship offers potential applications in reliability-based design and uncertainty quantification, enabling more efficient structural analysis and optimization under material randomness.

Acknowledgement

This research is funded by University of Transport and Communications (UTC) under grant number T2025-PHII_CT-006.

References

Ariaratnam, T. and Schuëller, G.I. (2020), *Stochastic Structural Dynamics: Progress in Theory and Applications*, CRC Press, London.

Arregui-Mena, J.D., Margetts, L. and Mummery, P.M. (2016), "Practical application of the stochastic finite element method", *Arch. Comput. Meth. Eng.*, **23**(1), 171-190. https://doi.org/10.1007/s11831-014-9139-3.

Bastian, C.D. and Rabitz, H. (2020), "Uncertainty quantification by random measures and fields", ArXiv.

Blatman, G. and Sudret, B. (2011), "Adaptive sparse polynomial chaos expansion based on least angle regression", *J. Comput. Phys.*, **230**(6), 2345-2367. https://doi.org/10.1016/j.jcp.2010.12.021.

Bozkurt, S., Abed, A. and Karstunen, M. (2023), "Finite element analysis for a deep excavation in soft clay supported by lime-cement columns", *Comput. Geotech.*, **162**, 105687. https://doi.org/10.1016/j.compgeo.2023.105687.

Cao, X., Xu, Y., Kong, Z., Shen, H. and Zhong, W. (2017), "Residual stress of 800MPa high strength steel welded T section: Experimental study", *J. Constr. Steel Res.*, **131**, 30-37. https://doi.org/10.1016/j.jcsr.2016.12.001.

Chen, X., Li, D., Tang, X. and Liu, Y. (2021), "A three-dimensional large-deformation random finite-element study of landslide runout considering spatially varying soil", *Landslid.*, **18**(9), 3149-3162. https://doi.org/10.1007/s10346-021-01699-1.

Das, S. and Roy, K. (2023), "Propagation of material uncertainty in modal parameters and its influence in damage quantification of shear buildings", *Prob. Eng. Mech.*, **74**, 103539. https://doi.org/10.1016/j.probengmech.2023.103539.

Deodatis, G. (1991), "Weighted integral method. I: Stochastic stiffness matrix", *J. Eng. Mech.*, **117**(8), 1851-1864. https://doi.org/10.1061/(ASCE)0733-9399(1991)117:8(1851.

Der Kiureghian, A. and Ke, J.B. (1988), "The stochastic finite element method in structural reliability", *Prob. Eng. Mech.*, **3**(2), 83-91. https://doi.org/10.1016/0266-8920(88)90019-7.

Du, W., Ma, J., Zhou, C., Yan, Y. and Wriggers, P. (2023), "Uncertain dynamic characteristic analysis for structures with spatially dependent random system parameters", *Mater.*, **16**(3), 1188. https://doi.org/10.3390/ma16031188.

Elishakoff, I. and Ren, Y. (2003), *Finite Element Methods for Structures with Large Stochastic Variations*, OUP Oxford, New York.

Fonseca, E.M. (2024), "Steel columns under compression with different sizes of square hollow cross-sections, lengths, and end constraints", *Appl. Sci.*, **14**(19), 8668. https://doi.org/10.3390/app14198668.

Fu, Q., Liu, J., Shi, J., Li, X., Cai, X. and Meng, Z. (2022), "Uncertainty evaluation of stochastic structural response with correlated random variables", *Shock Vib.*, **2022**(1), 1496358. https://doi.org/10.1155/2022/1496358.

Ganesan, R. and Kowda, V.K. (2005), "Buckling of composite beam-columns with stochastic properties", *J. Reinf. Plast. Compos.*, **24**(5), 513-543. https://doi.org/10.1177/0731684405045017.

Grigoriu, M. (1993), "On the spectral representation method in simulation", *Prob. Eng. Mech.*, **8**(2), 75-90. https://doi.org/10.1016/0266-8920(93)90002-D.

Hang, D., Nguyen, X. and Tien, D. (2022), "Stochastic buckling analysis of non-uniform columns using stochastic finite elements with discretization random field by the point method", *Eng. Technol. Appl. Sci. Res.*, **12**(2), 8458-8462. https://doi.org/10.48084/etasr.4819.

Hurtado, J.E. and Barbat, A.H. (1998), "Monte Carlo techniques in computational stochastic mechanics", *Arch. Comput. Meth. Eng.*, **5**(1), 3-29. https://doi.org/10.1007/BF02736747.

Jamaluddin, N., Lam, D., Dai, X.H. and Ye, J. (2013), "An experimental study on elliptical concrete filled columns under axial compression", *J. Constr. Steel Res.*, **87**, 6-16. https://doi.org/10.1016/j.jcsr.2013.04.002.

Jiang, D., Bechle, N.J., Landis, C.M. and Kyriakides, S. (2016), "Buckling and recovery of NiTi tubes under axial compression", *Int. J. Solid. Struct.*, **80**, 52-63. https://doi.org/10.1016/j.ijsolstr.2015.10.022.

Johari, A. and Talebi, A. (2021), "Stochastic analysis of piled-raft foundations using the random finite-element method", *Int. J. Geomech.*, **21**(4), 04021020. https://doi.org/10.1061/(ASCE)GM.1943-5622.0001966.

Jothimani, B. and Umarani, C. (2019), "Experimental investigation on concrete filled steel tubular column to foundation connections subjected to combined axial and lateral cyclic loading", *Lat. Am. J. Solid. Struct.*, **16**, e202. https://doi.org/10.1590/1679-78255629.

Kala, Z., Valeš, J. and Jönsson, J. (2017), "Random fields of initial out of straightness leading to column buckling", *J. Civil Eng. Manage.*, **23**(7), 902-913. https://doi.org/10.3846/13923730.2017.1341957.

Kamiński, M. (2022), "Uncertainty analysis in solid mechanics with uniform and triangular distributions using stochastic perturbation-based finite element method", *Finite Elem. Anal. Des.*, **200**, 103648. https://doi.org/10.1016/j.finel.2021.103648.

Kowda, V.K. (2002), "Free-vibration and buckling of prismatic and thin-walled composite beam-columns with stochastic properties", Concordia University.

Krejsa, M. and Kralik, J. (2015), "Probabilistic computational methods in structural failure analysis", *J. Multisc. Model.*, **06**(03), 1550006. https://doi.org/10.1142/S1756973715500067.

Liu, W.K., Belytschko, T. and Mani, A. (1986), "Probabilistic finite elements for nonlinear structural dynamics", *Comput. Meth. Appl. Mech. Eng.*, **56**(1), 61-81. https://doi.org/10.1016/0045-7825(86)90136-2.

Liu, X., Liu, J., Zhao, Y., Nie, Y., Liu, J. and Ding, T. (2024), "A Bayesian deep learning-based adaptive wind farm power prediction method within the entire life cycle", *IEEE Trans. Sustain. Energy*, **15**(4), 2663-2674. https://doi.org/10.1109/TSTE.2024.3435936.

Lobo, L.V. (2024), "Julia language implementation of the finite element method for linear instability of plane frames: An efficient alternative for structural analysis", *Lat. Am. J. Solid. Struct.*, **21**(3), e542. https://doi.org/10.1590/1679-78257958.

Ly, H.B., Desceliers, C., Minh Le, L., Le, T.T., Thai Pham, B., Nguyen-Ngoc, L., Doan, V.T. and Le, M. (2019), "Quantification of uncertainties on the critical buckling load of columns under axial compression with uncertain random materials", *Mater.*, **12**(11), 1828. https://doi.org/10.3390/ma12111828.

Ma, T.Y., Liu, X., Hu, Y.F., Chung, K.F. and Li, G.Q. (2018), "Structural behaviour of slender columns of high strength S690 steel welded H-sections under compression", *Eng. Struct.*, **157**, 75-85. https://doi.org/10.1016/j.engstruct.2017.12.006.

Najafian Jazi, F., Mir Mohammad Hosseini, S.M., Ghasemi-Fare, O. and Rockaway, T.D. (2024), "Experimental evaluation of stress history effect on compressibility characteristics of lime-stabilized expansive soils", *Geomech. Geoeng.*, **20**(1), 21-34. https://doi.org/10.1080/17486025.2024.2354873.

Nath, K., Dutta, A. and Hazra, B. (2019), "An iterative polynomial chaos approach toward stochastic elastostatic structural analysis with non-Gaussian randomness", *Int. J. Numer. Meth. Eng.*, **119**(11), 1126-1160. https://doi.org/10.1002/nme.6086.

Nguyen, H.X., Ta, H.D., Lee, J. and Nguyen-Xuan, H. (2017), "Stochastic buckling behaviour of laminated composite structures with uncertain material properties", *Aerosp. Sci. Technol.*, **66**, 274-283. https://doi.org/10.1016/j.ast.2017.01.028.

Nouy, A. (2009), "Recent developments in spectral stochastic methods for the numerical solution of stochastic partial differential equations", *Arch. Comput. Meth. Eng.*, **16**(3), 251-285. https://doi.org/10.1007/s11831-009-9034-5.

Pascual, B. and Adhikari, S. (2012), "A reduced polynomial chaos expansion method for the stochastic finite element analysis", *Sadhana*, **37**(3), 319-340. https://doi.org/10.1007/s12046-012-0085-1.

Pulsipher, J.L., Davidson, B.R. and Zavala, V.M. (2022), "Random field optimization", *Comput. Chem. Eng.*, **165**, 107854. https://doi.org/10.1016/j.compchemeng.2022.107854.

Quang, N.D., Cuong, N.H. and Tien, N.D. (2020), "Experimental and analyticalevaluation of concentrically

loadedreinforced concrete columns strengthening by carbon textile reinforced concrete jacketing", *Transp. Commun. Sci. J.*, **71**(5), 486-499. https://doi.org/10.25073/tcsj.71.5.3.

Ramu, S.A. and Ganesan, R. (1992), "Stability of stochastic Leipholz column with stochastic loading", *Arch. Appl. Mech.*, **62**(6), 363-375. https://doi.org/10.1007/BF00804597.

Salazar, F. and Hariri-Ardebili, M.A. (2022), "Coupling machine learning and stochastic finite element to evaluate heterogeneous concrete infrastructure", *Eng. Struct.*, **260**, 114190. https://doi.org/10.1016/j.engstruct.2022.114190.

Saouma, V.E. and Hariri-Ardebili, M.A. (2021), *Probabilistic and Random FEM*, Springer International Publishing, Cham.

Sasikumar, P., Suresh, R. and Gupta, S. (2014), "Stochastic finite element analysis of layered composite beams with spatially varying non-Gaussian inhomogeneities", *Acta Mechanica*, **225**(6), 1503-1522. https://doi.org/10.1007/s00707-013-1009-9.

Schuëller, G.I. and Pradlwarter, H.J. (2007), "Benchmark study on reliability estimation in higher dimensions of structural systems–An overview", *Struct. Saf.*, **29**(3), 167-182. https://doi.org/10.1016/j.strusafe.2006.07.010.

Schuëller, G.I. and Pradlwarter, H.J. (2009), "Uncertain linear systems in dynamics: Retrospective and recent developments by stochastic approaches", *Eng. Struct.*, **31**(11), 2507-2517. https://doi.org/10.1016/j.engstruct.2009.07.005.

Shinozuka, M. and Deodatis, G. (1991), "Simulation of stochastic processes by spectral representation", *Appl. Mech. Rev.*, **44**(4), 191-204. https://doi.org/10.1115/1.3119501.

Shinozuka, M. and Deodatis, G. (1996), "Simulation of multi-dimensional gaussian stochastic fields by spectral representation", *Appl. Mech. Rev.*, **49**(1), 29-53. https://doi.org/10.1115/1.3101883.

Stefanou, G. (2009), "The stochastic finite element method: Past, present and future", *Comput. Meth. Appl. Mech. Eng.*, **198**(9), 1031-1051. https://doi.org/10.1016/j.cma.2008.11.007.

Sudret, B., Berveiller, M. and Lemaire, M. (2020), *Application of a Stochastic Finite Element Procedure to Reliability Analysis*, CRC Press, England.

Ta, H.D. (2020), "A static analysis of nonuniform column by stochastic finite element method using weighted integration approach", *Transp. Commun. Sci. J.*, **70**(4), 359-367. https://doi.org/10.25073/tcsj.71.4.5.

Ta, H.D. and Nguyen, P.C. (2020), "Perturbation based stochastic isogeometric analysis for bending of functionally graded plates with the randomness of elastic modulus", *Lat. Am. J. Solid. Struct.*, **17**(07), e306. https://doi.org/10.1590/1679-78256066.

Tien, N.D. and Van, P.P. (2023), "Moment modification factors for the buckling design of steel beams – new recommendations", *Transp. Commun. Sci. J.*, **74**(1), 10-19. https://doi.org/10.47869/tcsj.74.1.2

Troian, R. (2023), "Uncertainty analysis of structural response under a random impact", *Optimiz. Eng.*, **24**(1), 49-64. https://doi.org/10.1007/s11081-021-09596-1.

Van den Nieuwenhof, B. and Coyette, J.P. (2003), "Modal approaches for the stochastic finite element analysis of structures with material and geometric uncertainties", *Comput. Meth. Appl. Mech. Eng.*, **192**(33), 3705-3729. https://doi.org/10.1016/S0045-7825(03)00371-2.

Wang, Y., Lyu, B., Shi, C. and Hu, Y. (2024), "Non-parametric simulation of random field samples from incomplete measurements using generative adversarial networks", *Georisk: Assess. Manage. Risk Eng. Syst. Geohazard.*, **18**(1), 60-84. https://doi.org/10.1080/17499518.2023.2222383.

Wu, Z., Huang, B., Fan, J. and Chen, H. (2023), "Homotopy based stochastic finite element model updating with correlated static measurement data", *Measure.*, **210**, 112512. https://doi.org/10.1016/j.measurement.2023.112512.

Yang, B., Shen, L., Kang, S.B., Elchalakani, M. and Nie, S.D. (2018), "Load bearing capacity of welded Q460GJ steel H-columns under eccentric compression", *J. Constr. Steel Res.*, **143**, 320-330. https://doi.org/10.1016/j.jcsr.2018.01.011.

Yang, H., Feng, S., Hao, P., Ma, X., Wang, B., Xu, W. and Gao, Q. (2022), "Uncertainty quantification for initial geometric imperfections of cylindrical shells: A novel bi-stage random field parameter estimation method", *Aerosp. Sci. Technol.*, **124**, 107554. https://doi.org/10.1016/j.ast.2022.107554.

Zhang, J. and Ellingwood, B. (1994), "Orthogonal series expansions of random fields in reliability analysis", *J. Eng. Mech.*, **120**(12), 2660-2677. https://doi.org/10.1061/(ASCE)0733-9399(1994)120:12(2660).

Zhao, H., Wang, C. and Fan, J. (2024), "Predicting steel column stability with uncertain initial defects using bayesian deep learning", *Appl. Soft Comput.*, **151**, 111139. https://doi.org/10.1016/j.asoc.2023.111139.

Zhao, H., Zhang, Y., Zhu, W., Fu, C. and Lu, K. (2024), "A comprehensive study on seismic dynamic responses of stochastic structures using sparse grid-based polynomial chaos expansion", *Eng. Struct.*, **306**, 117753. https://doi.org/10.1016/j.engstruct.2024.117753.

Zheng, Y., Chen, Z., Liu, B., Li, P., Huang, J., Chen, Z. and Xiang, J. (2024), "Robust topology optimization for multi-material structures considering material uncertainties", *Thin Wall. Struct.*, **201**, 111990. https://doi.org/10.1016/j.tws.2024.111990.

Zhou, K., Wang, Z., Gao, Q., Yuan, S. and Tang, J. (2023), "Recent advances in uncertainty quantification in structural response characterization and system identification", *Prob. Eng. Mech.*, **74**, 103507. https://doi.org/10.1016/j.probengmech.2023.103507.